Comparison of Two Transverse Flux Machines for an Aerospace Application

Steven Jordan, Nick J. Baker
Electrical Power Group, Newcastle University, Newcastle, United Kingdom

***Abstract*— More-electric is a platform being widely adopted by the current generation of aircraft. It offers significant benefits in terms of fuel savings and flexibility of airframe design, as well as passenger comfort. The application of a motor drive to facilitate an aircraft's on-ground operations has been well studied but as yet no solution has come to market for civil aerospace. This paper documents a transverse flux machine topology for use in short-haul aircraft, where current inefficiency can be bettered through use of an electrical machine. Simulation results are presented for two machine designs using different approaches to the challenging specification. Information regarding the challenges associated with building such a machine design are also discussed.**

Keywords—Aerospace, Transverse Flux

I. INTRODUCTION

The aerospace industry is under increasing pressure to significantly reduce emissions, fuel consumption and noise. This has led to focus on the more-electric aircraft, where functions currently carried out by the main engines or auxiliary systems can instead make use of efficient electric drives. However, the location of motors for more-electric aircraft can provide some significant challenges due to existing airframe design. This paper considers an application with a medium-term operating cycle based on a short-haul flight cycle involving a hub-type airport.

This paper describes the development of an electric motor which is believed to give a potential fuel mass saving of 396 kg per flight in a medium sized, twin engine, passenger aircraft: this equates to a saving of approximately 158 tonnes of CO_2 annually. This benefit is sensitive to the mass of the proposed motor: too heavy and the fuel burn during the flight cycle will negate any potential savings made, too little active material and the machine will saturate early, which will limit torque production. Moreover, a low mass solution will be thermally challenged. The target is toward a retrospective fitment; thus the mass and performance must be sustainable to the infrastructure already in place. It can be observed, therefore, that torque density is key in this area and thermal consideration is necessary.

To meet rated torque conditions, cooling during operation is vital: the application sustains a high load, and, consequently, requires a high current to develop the necessary air-gap shear stress. Thermal relief can only be provided by means of natural or forced-air cooling, where liquid cooling is not suitable due to safety, mass and maintenance restrictions. In order to account for any shock loads there is a constraint on the machine air-gap, which will impact on torque production. Furthermore, there is an overspeed condition where the speed of the motor will be far in excess of its operating point, leading to a significant back-emf developed: the converter must be adequately protected to avoid component failure.

Technical comparisons can be drawn with other high torque density machines. Work carried out by Galea et al [1] demonstrates a radial flux machine topology, which was chosen to meet a torque requirement in excess of 6 kNm [2]. The solution posed had a generous spacial envelope which allowed for the end-windings without impinging greatly on the active material available to develop the high air-gap shear stresses required. Furthermore, the mass and the current density figures discussed are far in excess of those available for this application. A high torque density axial flux variant is discussed in [3] which uses soft magnetic composite (SMC) material to remove the yoke, reducing the active material mass and improving the torque density of the machine.

The design and construction of two air-cooled, high torque density machine topologies, both of which are transverse flux machines, are investigated for use in this aerospace application. Both prototypes utilize the same flux concentrated rotor, which has NdFeB N35EH magnets sandwiching SMC pole pieces: the first prototype uses SMC in its stator construction for the core-back, whilst the second prototype has an SMC-free stator design, using formed laminations to guide the magnetic flux. The stator for prototype 2, where considerable thermal and mechanical stresses occur, takes into account that SMC is not currently certified for use in aerospace, the common rotor topology does not.

II. PROTOTYPE DESIGN AND CONSTRUCTION

A. Specification

The specification for the application contains sensitive information and key data are therefore masked in this paper using per unit (p.u.) quantities, contained in *TABLE I.* . The volumetric envelope for the electric machine is based on available space. An existing converter is provided, the output of which acts as a constraint for the motor performance. Based on the spacial envelope, and the torque required in the specification, the optimal topology - selected through comparative study - was a transverse flux machine (TFM) [4]. Whilst the target rated and overload torque figures cannot be revealed, the magnitude of the rated torque density gives some indication as to the challenge that this machine design faces with no external cooling circuit available.

This project is funded by Innovate UK

TABLE I. POWER CONVERTER† AND MOTOR SPECIFICATION

	Value	Unit
Phases†	3	-
Voltage†	<215	V_{RMS}
Rating†	160	kVA
Speed	<450	rpm
Overload/Rated Torque Ratio	3.2:1	-
Min. Air-gap Length	1	mm
Torque Density	37.5	Nm/kg

B. *Rotor Design*

For this application, an outer rotor topology is highly suited, where the rotor magnets can interface the internal bore of the spacial envelope of the application. Furthermore, the maximum radial length will increase the shear force in the air-gap. TFMs are renowned for their high pole numbers due to the removal of the electrical and magnetic loading constraints typical in radial and axial flux machines. This limits the size of the magnets around the periphery of the machine such that surface mounted magnets are no longer attractive. Flux concentrated rotors offer a significant air-gap flux density without impinging greatly on the radial distance. However, the concentrated field, combined with the typically high pole number, produces a strong reluctance torque that leads to large cogging and ripple torque values. Due to the flux flow, the rotor pole pieces between the flux concentrating magnets are constructed from Höganäs' prototyping SMC. This material has a greater suitability for machining but sacrifices performance with a lower mass density leading to low permeability and saturation characteristics when compared with higher grade SMC suitable for pressing. However, it can be machined into more complex shapes, which allowed mass savings techniques to be applied [5]. A reduction in the size of the pole pieces allows for magnet shaping to provide 1% increase in average torque output but creates a greater ripple torque, which is already of concern for this machine type.

C. *First Prototype: SMC-Laminate*

Whilst optimising the rotor, the stator for the first prototype was subjected to a similar procedure. Tooth size and span was considered with respect to a design which could meet the stringent mass and torque targets set out in the specification. Since torque density was a key factor, maximising that aspect was critical in the design. Work carried out in [6] intimated that utilising a combined-phase structure - where adjacent phase teeth are combined to form a mutual path - yields a higher torque density, shown in *Fig. 1*. Controlling the ripple torque is difficult with TFMs: in traditional machine designs, smoothing the air-gap is a relatively straightforward process of controlling the slot size, magnet span and longitudinally skewing the stator or rotor. Skewing a permanent magnet rotor creates manufacturing complexity, particularly when there is a high pole number. The stator of a TFM can be skewed along its axial direction [7] or pitched by alternating the tooth space over two - or more - poles in the radial plane [8] to reduce the ripple effects. The former would require a complicated arrangement of laminates or, if SMC were to be used, a method of pressing the SMC components such that the pressure is even over the skew length where care must be taken with the tooth edges, which are prone to fragmenting. Pitching the teeth is, therefore, more readily achievable and, in this instance, with a laminated design, can be incorporated easily [5]. The laminations are made from silicon iron rather than high grade cobalt iron, saving cost due to their manufacturing method and the internal bore diameter leading to a large amount of waste material.

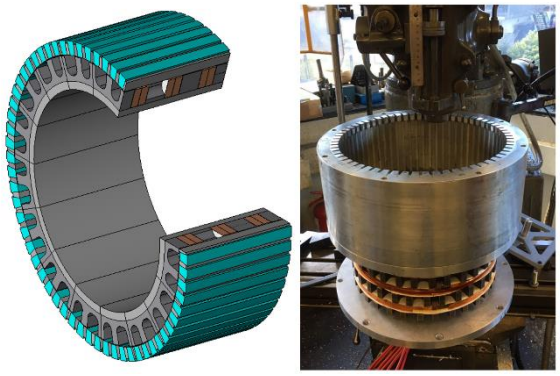

Fig. 1. (*l*) Prototype 1 SMC-Laminate JMAG Model and (*r*) Constructed Prototype Rotor and Stator

D. *Second Prototype: Formed Lamination*

The construction of the three-phase motor will mean a move away from the combined-phase design since the mutual flux paths no longer exist, depicted in *Fig. 2*. The forming of laminations will remove the need for an SMC core-back. Whilst SMC is retained in the rotor, it is removed from the thermal and mechanical extremes experienced by the stator, thus making it more suitable for use in applications where shock loads can be transferred through the stator. Work carried out in [9] details prototyping difficulties in performing bends with such tight radii and bonding the laminations. Accounting for these in the design of the second prototype, a bespoke support structure is considered to help retain the structure and provide a platform for forming the laminations. The structure retains the pitching of the teeth from the first prototype. Since each phase can be constructed separately, the laminations are formed from chains rather than pressed rings, therefore the laminated steel can be a higher grade, such as cobalt iron, due to the reduction in waste material.

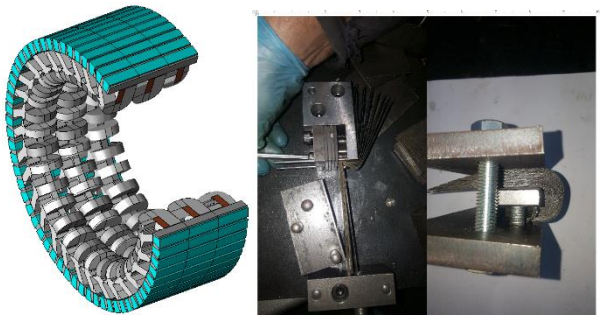

Fig. 2. (*l*) Prototype 2 Formed Lamination JMAG Model and (*r*) Forming of Stator Laminations

III. PERFORMANCE COMPARISON

The performance of the two machine designs is compared in this section with a consistent current density providing a reference benchmark. Key data are contained in *TABLE II.* , with further analysis described in greater detail in each subsection.

TABLE II. COMPARISON OF MACHINE PERFROMANCE

	Formed Lamination	SMC-Laminate
Average of Back-emf across 3ϕ (V)	115.1	87.8
RMS Cogging Torque (% of AVG rated)	5.12	4.89
Average Load Torque @ 6.5 A_{RMS}/mm^2 (p.u.)	0.81	1.09
Mass (p.u.)	1.48	1.67
Torque Density (Nm/kg)	20.5	24.5

A. *Cogging Torque*

The open-circuit simulations of the two machine topologies are compared below, revealing key differences in the two designs. The cogging torque depicted in *Fig. 3* highlights a variation in performance between the combined-phase and the separate-phase designs. Whilst both designs employ stator tooth pitching, the mutual flux paths in the combined-phase model negate some of the higher order harmonics present in the air-gap flux, where the separate-phase model reduces the magnitude of the 4th harmonic torque component by 55 % but exhibits a significant increase in the 12th and 20th harmonics.

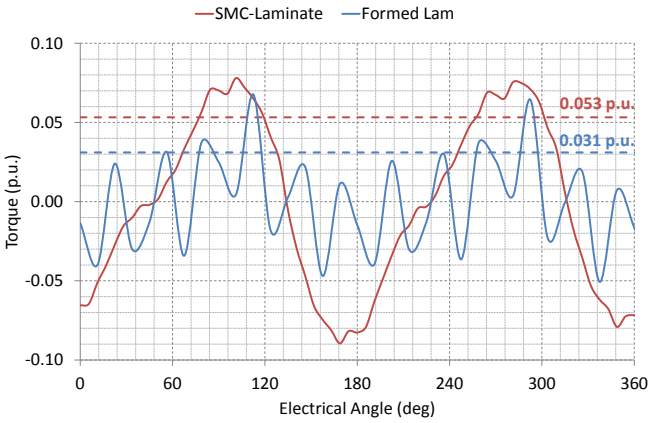

Fig. 3. Cogging Torque

B. *Back-emf*

The back-emf waveforms, depicted in *Fig. 4*, show a sinusoidal wave shape but reflect the increase in flux linkage in the central phase for both designs. The separate-phase design has the same issue as the combined-phase machine due to the rotor having no isolation between the phases, therefore, the central phase sees a higher rotor flux.

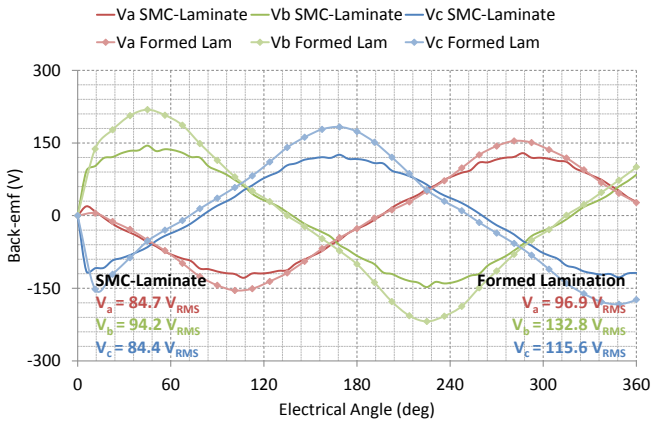

Fig. 4. Back-emf Waveforms

C. *Load Torque*

Since the rotor is axially fixed in length, the slot size for the formed lamination motor is much smaller than that of the laminated-SMC design due to the mutual flux paths reducing material. Under load conditions, comparisons of the machine performances are based on current densities. For rated conditions, a current density of 6.5 A_{RMS}/mm^2 is achieved for a low duty cycle, air-cooled machine. The load torque waveforms in *Fig. 5* demonstrate the decrease in performance for the formed lamination structure. However, the material savings yield a lower mass, improving its torque density.

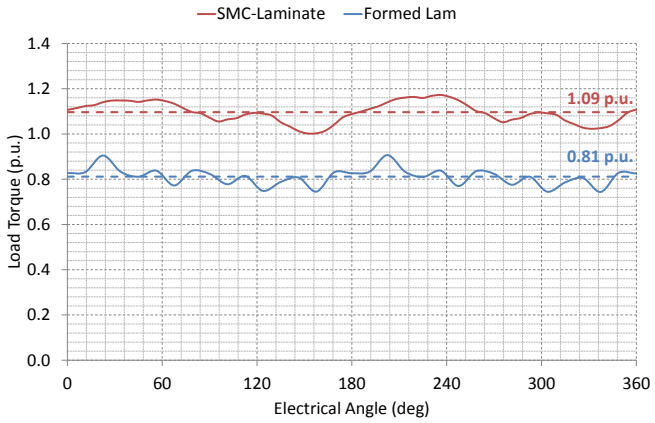

Fig. 5. Torque Output at 6.5 A_{RMS}/mm^2

Disappointing torque density figures, contained in *Table II*, can be accounted for through use of inferior materials due to budgetary constraints and the addition of air-gaps introduced during the fabrication process of the prototypes. With minimal manufacturing gaps in the rotor, cobalt iron, and high grade pressed Somaloy®, the torque density figure can be improved upon: up to 17 % for the SMC-Laminate machine.

D. *Overload Torque*

The overload target for this machine is over three times the rated torque output. Using a two coil per slot approach to satisfy mechanical constraints in terminating the windings provided

limitations on the first prototype's ability to meet overload torque. The voltage output from the converter, combined with the stringent mass target, limited the number of turns in the windings, which restricted the coil MMF. At full converter current then, the torque limit is achieved, depicted in *Fig. 6*.

However, for the second prototype, there is an ability to push the current higher, increasing the copper current density to 13 A_{RMS}/mm^2. For short duty applications it would be acceptable to run the machine with this level of thermal stress without an external cooling circuit to soak the heat away. However, reducing the current density to that of the first prototype would not yield the required rated torque, thus the second prototype would need to be run at a higher current density (8.4 A_{RMS}/mm^2) to meet the rated torque requirement. For full converter current, the torque output is shown in *Fig. 6*.

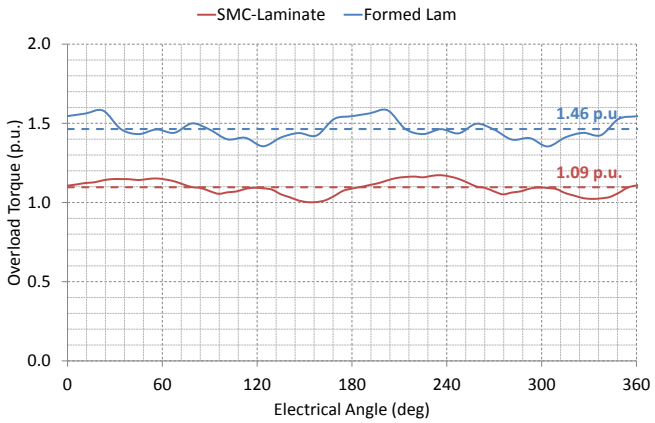

Fig. 6. Overload Capability of the Two Prototypes

E. Losses and Thermal Performance

Due to the low mass design of both of the motors, losses and their resultant thermal performance becomes important. For Joule losses, SMC is a good, low-loss material as a result of the small grain size limiting eddy current. However, at lower operating frequencies, the hysteresis losses are dominant, giving rise to the high loss values shown in *TABLE III.* .

TABLE III. AVERAGE OF COMPONENT LOSSES

	SMC-Laminate	Formed Lamination
Laminations (W)	25.98	155.6
Core-back (W)	172.4	N/A
Windings (W)	253.4	183.8
Magnets (W)	32.73	16.27
Pole Pieces (W)	97.08	25.03

From conductor, eddy current and hysteresis loss results, the heat generated in each component can be roughly calculated using equation (1):

$$\Delta T = Q/mc \quad (1)$$

where ΔT is the temperature rise, Q is the loss energy, m is the mass and c is the specific heat capacity of the material.

TABLE IV. CALCULATED TEMPERATURE RISES IN PROTOTYPE MOTORS

	SMC-Laminate	Formed Lamination
Laminations (°C)	71.6	120.2
Core-back (°C)	73.7	N/A
Windings (°C)	326.1	236.5
Magnets (°C)	36.6	68.6
Pole Pieces (°C)	211.9	133.3

The approximate component temperature rises calculated, shown in *TABLE IV.* , are not strictly comparable with the rises shown in *Fig. 7* since they do not account for interface boundaries dissipating heat. The coils depict a thermal difference due to losses in the central being high on account of the mutual flux linkage. The rotor poles and magnets interface with a significantly larger thermal mass, the rotor housing, which acts as a heat sink for the losses in these components.

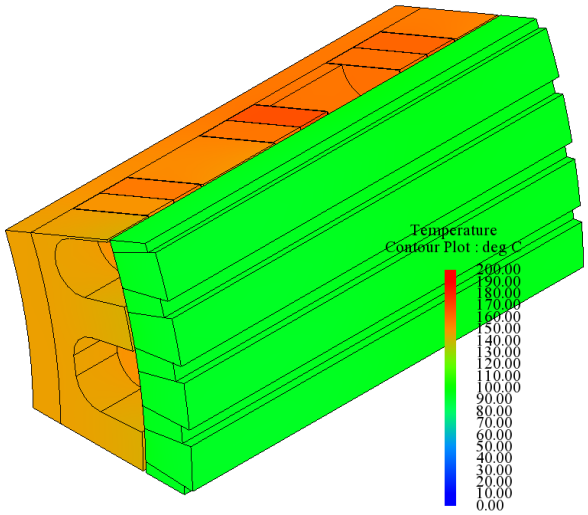

Fig. 7. Temperature Rise in Prototype 1 Over 30 Minutes with Zero Initial Conditions

IV. MANUFACTURING CHALLENGES

During prototyping, challenges were encountered in the fabrication of the two TFMs. This section details some of the significant issues in constructing a TFM of this size. Whilst the simulated results have been informed by the manufacturing process to ensure accuracy, the nature of these manufacturing differences are not as linear as the simulation set-up imposes: some components interface across small sections that may not be consistent across the entire face. Adding air-gaps to account for interface issues yields a reduction in torque output of 7.2 %.

A. Rotor

Small air-gaps between some component faces are difficult to avoid in the prototype construction, highlighted in *Fig. 8*. Due

to the tolerancing of the magnets and pole pieces requiring the allowance of an epoxy layer for bonding and possible misalignment in the rotor housing, the gaps are unavoidable. Furthermore, due to the cutting process employed, there is a thin oxidisation layer which was removed at the magnet interface surfaces but visible in *Fig. 8* prior to surface finishing of the central bore: removing high-spots and guaranteeing uniform air-gap length.

Fig. 8. Air-gaps Between Epoxy Retained Magnets and Pole Pieces

B. Stator

As with the rotor, the same issue of mechanical tolerance gaps exists at the interface of the SiFe laminations and the SMC core-back segments, where there are slight differences in arc profiles and re-strike channels from failure of the wire erosion. The manufacturing issues in bonding the laminations, depicted in *Fig. 9*, will lead to a loss of performance that cannot be readily simulated: they were rebonded where possible.

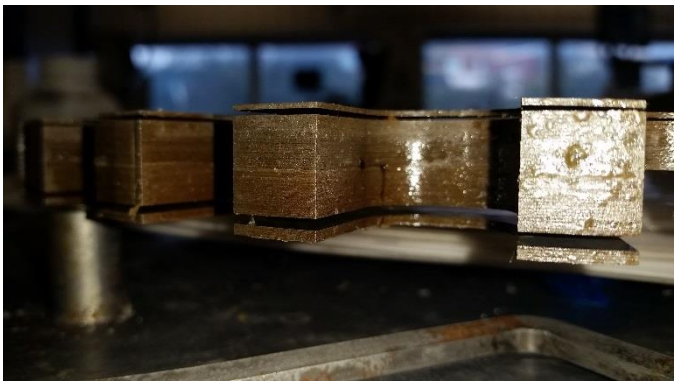

Fig. 9. Lamination Bonding Failure

C. Windings

The windings are simple toroidal coils, which were wound in situ when the stator core-back and laminate sections were formed together. For termination, and material availability reasons, the coil width was half of the available slot width, allowing two coils to be formed in each slot. Due to the large bend radius, the relative smoothness of the SMC and the thermal limitations placed on the machine, the coils were wound without a slot liner in place. However, short-circuits were present in all but two of the coils. The coils were removed and rewound with Nomex® slot liner in place. This solved the issues with the coil shorting to the machine body but the insulating effect of the Nomex® will have an impact on the thermal performance of the machine, incorporated in the simulation models.

The toroidal coils finish close to the air-gap of the stator and getting the coils to exit is difficult due to the external rotor topology. The initial approach was to solder the coils, allowing a right angle to be formed and a relatively straightforward bend to exit through the stator core-back. However, the thermal soaking capability of the structure resulted in the heat dissipating before the solder could take. It was, therefore, decided to use a mechanical termination means and copper clamps were fabricated to facilitate the coil exits, depicted in *Fig. 10*. Wires were then brought out of a central bore in the stator shaft. Copper busbars formed the star-point in the internal space of the machine.

Fig. 10. Copper Clamp for Coil Exit (*l*) and Busbar Star-point (*r*) Prior to Covering with Kapton® Insulating Tape

V. Conclusions

Two different methods of fabricating a transverse flux machine, for consideration in an aerospace application, are proposed with a varied approach to their design. The first prototype makes use of an SMC-laminate stator construction. As yet, SMC remains a material that is uncertified for use in aerospace, therefore, a second prototype is explored. The common rotor and first prototype use a grade of SMC that is suitable for prototyping, giving a lower performance than desired when simulated.

The converter provides a constraint that impinges the performance of the first prototype design. Furthermore, the mass target informs the thermal performance and, for 30 minute duty cycle, the current density can be sustained but without the ability to meet overload conditions. The second prototype provides some overload capability but at a greatly increased current density. The thermal performance is shown for the first prototype, which has higher losses compared with the second prototype.

Challenges encountered during the machine build are detailed and highlight possible performance issues arising from

manufacturing tolerances leading to air-gaps between components. Furthermore, bonding issues with laminations and coil winding ends are problematic.

ACKNOWLEDGMENT

The authors would like to thank to JSOL for providing the JMAG software, project partners Arnold Magnetics and MTD Ltd. for supplying and manufacturing materials, and Sharp Engineering, Merseyside, UK for their fabrication work.

REFERENCES

[1] M. Galea, T. Hamiti, and C. Gerada, "Torque Density Improvements for High Performance Machines," in IEEE International Electric Machines and Drives Conference, 2013, pp. 1066-1073.

[2] M. Galea, Z. Xu, C. Tighe, T. Hamiti, C. Gerada, and S. Pickering, "Development of an Aircraft Wheel Actuator for Green Taxiing," in International Conference on Electrical Machines, 2014, pp. 2492-2498.

[3] T. J. Woolmer and M. D. McCulloch, "Analysis of the Yokeless And Segmented Armature Machine," in 2007 IEEE International Electric Machines & Drives Conference, 2007, pp. 704-708.

[4] S. Jordan and N. J. Baker, "Air-Cooled, High Torque Machines for Aerospace Applications," in 8h IET Conference on Power Electronics, Machines and Drives, Glasgow, Scotland, UK, 2016.

[5] S. Jordan and N. J. Baker, "Design and build of a mass critical, air-cooled transverse flux machine for aerospace," in 2016 XXII International Conference on Electrical Machines (ICEM), 2016, pp. 1453-1458.

[6] J. G. Washington, G. J. Atkinson, N. J. Baker, A. G. Jack, B. C. Mecrow, B. B. Jensen, et al., "Three-Phase Modulated Pole Machine Topologies Utilizing Mutual Flux Paths," IEEE Transactions on Energy Conversion, vol. 27, pp. 507-515, 2012.

[7] F. Dreher and N. Parspour, "Reducing the Cogging Torque of PM Transverse Flux Machines by Discrete Skewing of a Segmented Stator," in 20th International Conference on Electrical Machines, 2012, pp. 454-457.

[8] J. G. Washington, G. J. Atkinson, and N. J. Baker, "Reduction of Cogging Torque and EMF Harmonics in Modulated Pole Machines," IEEE Transactions on Energy Conversion, vol. 31, pp. 759-768, 2016.

[9] E. Pinguey, "On the Design and Construction of Modulated Pole Machines," Power Electronics, Drives and Machines, Newcastle, 2010.